Detecting quasiperiodic structures with double diffraction

J. Xu and A. W. Hübler

Center for Complex Systems Research, Department of Physics, University of Illinois at Urbana-Champaign, Urbana, Illinois 61801

PACS 61.44.Br – Structure of quasicrystals
PACS 61.14.Dc – Theories of diffraction and scattering
PACS 33.40.+f – Multiple resonances

Abstract. - We study interference patterns of double diffraction systems with quasiperiodic structures. A quasiperiodic linear array of scatterers converts single delta pulses into a sequence of quasiperiodic pulses. This pulse train is diffracted from a second set of scatterers. We find that the interference pattern after the second diffraction has a pronounced peak if both sets of scatterers have similar quasiperiodic structures. We show that this method can be used for identifying the Fibonacci chain and related quasiperiodic sequences, if the number of scatterers in the first set is at least twice as large as the number of scatterers in the second set, and if the distances among the two sets of scatterers and the detector are all large compared to the size of the sets. This method may provide a methodology for identifying the structure of quasicrystals and quasiperiodic layered materials with a large signal to noise ratio.

Introduction. – Since the discovery of quasicrystal in 1984 [1], their diffraction patterns have been extensively studied both theoretically [2, 3] and experimentally [4–6]. Most of this work is based on hyperspace crystallography [7]. However standard X-ray diffraction experiments do not provide a unique structure, due to the local isomorphic nature of a quasilattice [8]. A similar ambiguity in identifying nonlinear dynamical systems can be resolved with aperiodic forcing functions [9–15]. More recent work shows that by using quasiperiodic pulse trains, it is possible to obtain diffraction patterns with only one major diffraction peak [17]. But the production of such a quasiperiodic pulse train is still an open question.

In this paper, we discuss a double diffraction technique, where a set of quasiperiodic scatterers creates a quasiperiodic pulse train, which is then used to identify the structure of a second set of quasiperiodic scatterers. The first set of point scatterers is called the source, the second set of scatterers is called the target. In a double diffraction system a single pulse plane wave is diffracted from the source. The diffracted wave forms a quasiperiodic pulse train in the far field. A screen prevents the quasiperiodic pulse train from reaching the detector. The pulse train is then diffracted from the target. After the quasiperiodic pulse train wave is diffracted from the target, it creates an interference pattern on the detector screen. We assume that there is a set of different sources, or that the structure of the source depends on an adjustable control parameter such as pressure or temperature. We repeat the double diffraction experiment with different source structures, until the interference pattern on the detector indicates that there is a perfect match between the structure of the source and the structure of the target. This may seem to be a simple procedure, however this procedure has a good signal to noise ratio for system identification only if the system parameters are well adjusted. Some of the important system parameters are the minimum number of scatterers in the source, the distance between the source and the target, and the distance between the target and the detector. In the following we discuss the adjustment of these and other parameters.

The double diffraction system. – We consider systems where the dynamics of the field $E(\mathbf{r}, t)$, at position $\mathbf{r}$ and time t is given by a linear wave equation

$$\frac{\partial E}{\partial t} - c^2 \nabla^2 E = 0 \tag{1}$$

where c is the wave speed and ∇^2 is the Laplacian operator in a d-dimensional space, and $d = 1, 2, \ldots$. The setup of the double diffraction technique is illustrated in fig. 1. The source is a linear arrangement of N_0 scatterers where the distances between the scatterers is an aperiodic sequence. The unit vector $\hat{\mathbf{R}}_0$ indicates the direction of the

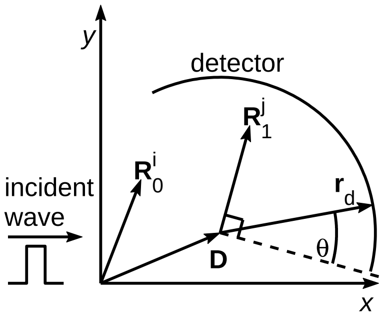

Fig. 1: Schematics of a double diffraction system. $\mathbf{R}_0^i$ indicates the direction of the source scatterers and $\mathbf{R}_1^j$ indicates the direction of the target scatterers. $\mathbf{D}$ is the displacement from the source scatterers to the target scatterers. θ is the diffraction angle.

source. $\mathbf{R}_0^i = R_0^i \hat{\mathbf{R}}_0$ is the position of the i'th source scatterer. The distribution function of the source scatterers is $L_0(\mathbf{r}) = \sum_{i=1}^{N_0} \frac{1}{\delta_s} \Pi(|\mathbf{R}_0^i - \mathbf{r}|/\delta_s)$, where δ_s is the size of the scatterer and Π is the rectangular function. The target is a linear arrangement of scatterers too, where the distances between the scatterers is typically a different aperiodic sequence. The unit vector $\hat{\mathbf{R}}_1$ indicates the direction of the target. $\mathbf{T}^j = \mathbf{D} + \mathbf{R}_1^j$ is the position of the j'th target scatterer, where $\mathbf{R}_1^j = R_1^j \hat{\mathbf{R}}_1$, $\mathbf{D} = D\hat{\mathbf{D}}$, and $\hat{\mathbf{D}}$ is a unit vector. The distribution function of the target scatterers is $L_1(\mathbf{r}) = \sum_{j=1}^{N_1} \frac{1}{\delta_s} \Pi(|\mathbf{D} + \mathbf{R}_1^j - \mathbf{r}|/\delta_s)$. The detector is located on a circle with radius r_d, centered at $\mathbf{D}$. $\mathbf{r}_d = r_d \hat{\mathbf{r}}_d$ is the vector from $\mathbf{D}$ to a location on the detector, where θ is the angle between a normal vector to the direction of the target scatterers and $\mathbf{r}_d$, -*i.e.* $\sin\theta = \hat{\mathbf{R}}_1 \cdot \hat{\mathbf{r}}_d$. θ is the diffraction angle. The quasiperiodic structure of the source and the target is constructed with the (P)roject (A)nd (C)ut procedure [17,18] with structural parameter α_0 and α_1 respectively:

$$R_0^i = \left(i + (\cot\alpha_0 - 1)\lfloor \frac{i}{1+\tan\alpha_0} \rfloor\right) a_0 \sin\alpha_0 \quad (2)$$

$$R_1^j = \left(j + (\cot\alpha_1 - 1)\lfloor \frac{j}{1+\tan\alpha_1} \rfloor\right) a_1 \sin\alpha_1 \quad (3)$$

where $i = 1\ldots N_0$ and $j = 1\ldots N_1$. N_0, N_1 are the numbers of source scatterers and target scatterers respectively. The parameters a_0 and a_1 adjust the distance between neighboring scatterers. In the source the distance between neighboring scatterers is either $A_0 = a_0 \sin\alpha_0$ or $B_0 = a_0 \cos\alpha_0$, and $A_1 = a_1 \sin\alpha_1$ or $B_1 = a_1 \cos\alpha_1$ in the target. Hence $R_0^i = \sum_{k=0}^{i} A_0 + (B_0 - A_0)s_0^k$ and $R_1^j = \sum_{k=0}^{j} A_1 + (B_1 - A_1)s_1^k$ are weighted partial sums of the binary sequences $S_0 = \{s_0^1 s_0^2 \cdots s_0^{N_0-1}\}$ and $S_1 = \{s_1^1 s_1^2 \cdots s_1^{N_1-1}\}$, such as $S_0 = \{00100101\cdots\}$ and $S_1 = \{01000010\cdots\}$. In general, $\alpha_0 \neq \alpha_1$, thus the two sequences S_0 and S_1 are different. The average spacing between two scatterers is $\bar{l}_n = A_n\tau_n/(1+\tau_n) + B_n/(1+\tau_n) = a_n\sqrt{1+\tau_n^2}/(1+\tau_n)$, where $n = 0, 1$ and $\tau_n = \cot\alpha_n$. Hence the expectation value of the size of the source is $\bar{R}_0^{N_0} = N_0 a_0 \sqrt{1+\tau_0^2}/(1+\tau_0)$ and the expectation value of the size of the target is $\bar{R}_1^{N_1} = N_1 a_1 \sqrt{1+\tau_1^2}/(1+\tau_1)$. If a τ value is the golden mean $\tau_n = (1+\sqrt{5})/2$, then the corresponding sequence S_n is the Fibonacci Chain [19]. In our numerical simulations the target scatterers are a Fibonacci chain, -*i.e.* $\tau_1 = (1+\sqrt{5})/2$.

$\hat{\mathbf{k}} = (1, 0)$ is the direction of the wave vector of the incident wave. The incident wave is a delta pulse of height E_0 and duration δ, -*i.e.* the field of the incident wave is $E_I(\mathbf{r}, t) = E_0 \Pi((t - \mathbf{r}\cdot\hat{\mathbf{k}}/c)/\delta)$. We consider systems where $\hat{\mathbf{k}}$, $\hat{\mathbf{R}}_0$, $\hat{\mathbf{R}}_1$, and $\hat{\mathbf{D}}$ are coplanar.

In the numerical experiment we change the structural parameter of the source α_0 systematically and keep the structural parameter of the target α_1 constant. In a system identification experiment the structural parameter of the source is assumed to be known, whereas the structural parameter of the target is unknown. The field diffracted from the source is

$$E_s(\mathbf{r}, t) = \int C E_I(\tilde{\mathbf{r}}, \tilde{t}) L_0(\tilde{\mathbf{r}}) G(\mathbf{r}, t, \tilde{\mathbf{r}}, \tilde{t}) d\tilde{\mathbf{r}} d\tilde{t} \quad (4)$$

where C is the scattering strength of each scatterer, and $G(\mathbf{r}, t, \tilde{\mathbf{r}}, \tilde{t}) = \delta(\tilde{t} - t - |\mathbf{r} - \tilde{\mathbf{r}}|/c)/|\mathbf{r} - \tilde{\mathbf{r}}|^{d-1}$ is the propagator for eq. (1). If the target is far from the source ($D \gg \bar{R}_0^{N_0}$), and if the size of the scatterers is small ($\delta_s \ll \bar{R}_0^{N_0}/N_0$), E_s is a pulse train of planar waves near the target

$$\begin{aligned} E_s(\mathbf{r}, t) &\approx \sum_{i=1}^{N_0} \frac{C}{r^{d-1}} E_I(0, t - \frac{((\mathbf{r} - \mathbf{R}_0^i)\cdot\mathbf{r}/r + \mathbf{R}_0^i\cdot\hat{\mathbf{k}})}{c}) \\ &= \frac{CE_0}{r^{d-1}} \sum_{i=1}^{N_0} \Pi(\frac{t}{\delta} - \frac{r - R_0^i(\hat{\mathbf{R}}_0\cdot\hat{\mathbf{k}} - \hat{\mathbf{R}}_0\cdot\mathbf{r}/r)}{c\delta}) \\ &\approx c_1 \sum_{i=1}^{N_0} \Pi((r - R_0^i c_3 + c_4)/c_2) \end{aligned} \quad (5)$$

where $c_1 = CE_0/D^{d-1}$, $c_2 = -c\delta$, $c_3 = \hat{\mathbf{R}}_0\cdot\hat{\mathbf{k}} - \hat{\mathbf{R}}_0\cdot\hat{\mathbf{D}}$, $c_4 = ct$, and $r = |\mathbf{r}|$. The space dependence of the distribution function of the source (in the direction of the source) $L_0(r\hat{\mathbf{R}}_0) = \frac{1}{\delta_s}\sum_{i=1}^{N_0} \Pi((|\mathbf{r}| - R_0^i)/\delta_s)$, and the space dependence of the pulse train (in the direction of the target scatterers) $E_s(r\hat{\mathbf{D}})$ is the same, except for the magnitude c_1 and length of the pulses c_2, the change in length of the pulse train by the factor c_3, and a displacement c_4. The distances of the pulses in the pulse train have one of the two values $\tilde{A}_0 = A_0(\hat{\mathbf{R}}_0\cdot\hat{\mathbf{k}} - \hat{\mathbf{R}}_0\cdot\hat{\mathbf{D}})$ and $\tilde{B}_0 = B_0(\hat{\mathbf{R}}_0\cdot\hat{\mathbf{k}} - \hat{\mathbf{R}}_0\cdot\hat{\mathbf{D}})$. The pulses may overlap if their separation is less than the pulse length, -*i.e.* $\max\{A_0, B_0\} < \delta$, or $\max\{\sin\alpha_0, \cos\alpha_0\}|(\hat{\mathbf{R}}_0\cdot\hat{\mathbf{k}} - \hat{\mathbf{R}}_0\cdot\hat{\mathbf{D}})| < \delta/a_0$.

Time dependence of the field at the detector. – The field at the detector is the sum of the contributions

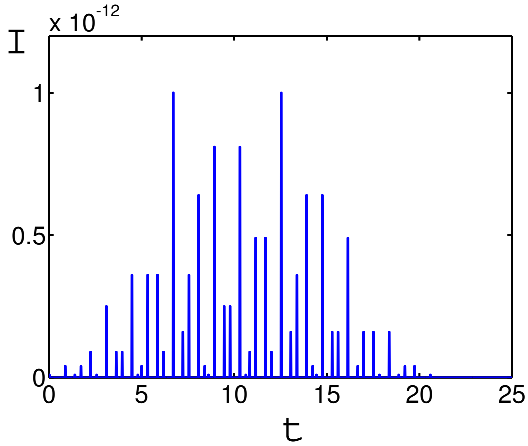

Fig. 2: A typical time dependence of the intensity of the field I at the detector.

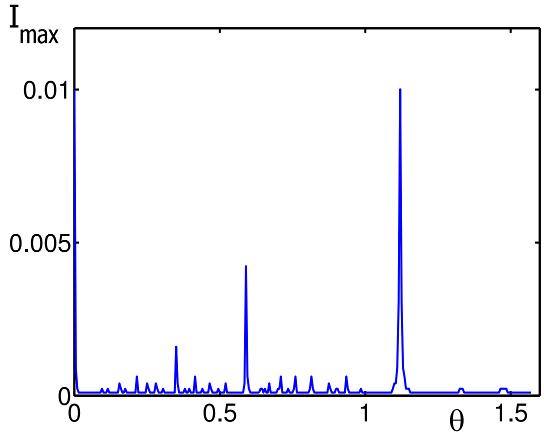

Fig. 3: The maximum intensity versus the diffraction angle for a double diffraction system, where both the source scatterers and the target scatterers are Fibonacci chains. The number of source scatterers $N_0 = 20$, and the number of target scatterers is $N_1 = 10$. The scaling parameters of the scatterers are $a_0 = 0.9$ and $a_1 = 1$. The location of the diffraction peak is close to the theoretical value $\theta_{max} = \arcsin(a_0/a_1) \approx 1.12$. The height of the main diffraction peak is close to the theoretical value $I_{max} = 0.01x10^{-10}$

from all the target scatterers

$$
\begin{aligned}
E_d(\mathbf{r}_d, t) &= \int C E_s(\tilde{\mathbf{r}}, \tilde{t}) L_r(\tilde{\mathbf{r}}) G(\mathbf{D} + \mathbf{r}_d, t, \tilde{\mathbf{r}}, \tilde{t}) d\tilde{\mathbf{r}} d\tilde{t} \\
&\approx \sum_{j=1}^{N_1} \frac{C}{|\mathbf{r}_{-}\mathbf{R}_1^j|} E_s(\mathbf{R}_1^j + \mathbf{D}, t - \frac{|\mathbf{r}_d - \mathbf{R}_1^j|}{c}) \qquad (6)
\end{aligned}
$$

if the size of the target scatterers is small. Since $\mathbf{r}_d$ is a function of the diffraction angle θ, the field at the detector is a function of the diffraction angle, *-i.e.* $E_d(\mathbf{r}_d, t) = E_d(\theta, t)$. We express the field at the detector in terms of the incident wave at the origin and the diffraction angle:

$$
\begin{aligned}
& E_d(\theta, t) = \\
& \sum_{i,j=1}^{N_0,N_1} \frac{C^2}{|\mathbf{r}_d(\theta) - \mathbf{R}_1^j|^{d-1} |\mathbf{R}_1^j + \mathbf{D} - \mathbf{R}_0^i|^{d-1}} \times \\
& E_I \left(0, t - \frac{|\mathbf{r}_d(\theta) - \mathbf{R}_1^j| + |\mathbf{R}_1^j + \mathbf{D} - \mathbf{R}_0^i| + \mathbf{R}_0^i \cdot \hat{\mathbf{k}}}{c} \right) \\
& = \sum_{i,j=1}^{N_0,N_1} \frac{C^2 E_0}{|\mathbf{r}_d(\theta) - \mathbf{R}_1^j|^{d-1} |\mathbf{R}_1 + \mathbf{D} - \mathbf{R}_0|^{d-1}} \times \\
& \Pi \left(\frac{t}{\delta} - \frac{|\mathbf{r}_d(\theta) - \mathbf{R}_1^j| + |\mathbf{R}_1^j + \mathbf{D} - \mathbf{R}_0^i| + \mathbf{R}_0^i \cdot \hat{\mathbf{k}}}{c\delta} \right) \\
& \approx \sum_{i,j=1}^{N_0,N_1} \frac{C^2 E_0}{(r_d D)^{d-1}} \times \qquad (7) \\
& \Pi \left(\frac{t}{\delta} - \frac{|\mathbf{r}_d(\theta) - \mathbf{R}_1^j| + |\mathbf{R}_1^j + \mathbf{D} - \mathbf{R}_0^i| + \mathbf{R}_0^i \cdot \hat{\mathbf{k}}}{c\delta} \right)
\end{aligned}
$$

Figure 2 shows the typical time dependence of the intensity of the field $I(t) = E_d^2(\theta, t)$ at the detector for $d = 2$, where $\hat{\mathbf{R}}_0 \cdot \hat{\mathbf{k}} = 0$, $\hat{\mathbf{R}}_0 = \hat{\mathbf{D}}$, and $\hat{\mathbf{R}}_1 = -\hat{\mathbf{k}}$. The distance between two scatterers is $D = 10^5$. The distance from the target detector to the screen is $r = 10^4$. The wave speed is $c = 1$, the amplitude of the original delta pulse $E_0 = 100$, and the width of the delta pulse $\delta = 0.02$. The detector placed at $\theta = \pi/2$ and the structural parameters of the source and target scatterers are $\tau_0 = \tau_1 = (1 + \sqrt{5})/2$ and $a_0 = a_1 = 1$. The scattering intensity is $C = 1$.

Diffraction patterns. – If the sequence of target S_1 is a subsequence of the source S_0, then constructive interference from all N_1 target scatterers occurs at the diffraction angle

$$
\theta_{max} = \arcsin(\hat{\mathbf{R}}_1 \cdot \hat{\mathbf{D}} + (\hat{\mathbf{R}}_0 \cdot \hat{\mathbf{k}} - \hat{\mathbf{R}}_0 \cdot \hat{\mathbf{D}}) \frac{a_0}{a_1}) \qquad (8)
$$

Figure 3 shows the maximum intensity $I_{max} = \max_t(E_d(\theta, t)^2)$ versus the diffraction angle θ for the system described in fig. 2, except that $a_0 = 0.9$. The diffraction pattern has a pronounced peak at the diffraction angle $\theta_{max} = \arcsin(a_0) \approx 1.12$. If there is constructive interference from all target scatterers the maximum intensity at the detector is

$$
I_{max} \approx \left(N_1 \frac{C^2 E_0}{(rD)^{d-1}} \right)^2 \qquad (9)
$$

The numerical value in fig. 3 agrees well with the theoretical value $I_{max} = 10^{-12}$. For a double diffraction systems $\hat{\mathbf{R}}_0 \cdot \hat{\mathbf{k}} = 0$, $\hat{\mathbf{R}}_0 = \hat{\mathbf{D}}$, and $\hat{\mathbf{R}}_1 = -\hat{\mathbf{k}}$ and $\theta = \theta_{max}$ eq. (7) simplifies to

$$
\begin{aligned}
E_d &= \frac{C^2 E_0}{(r_d D)^{d-1}} \times \\
& \sum_{i,j=1}^{N_0,N_1} \Pi \left(\frac{t}{\delta} - \frac{r_d + R_1^j + \sqrt{(R_1^j)^2 + (D - R_0^i)^2}}{c\delta} \right)
\end{aligned}
$$

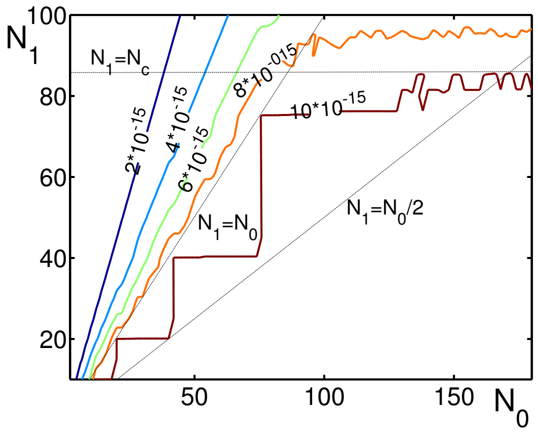

Fig. 4: The contour plot of the relative intensity I_{max}/N_1^2 vs. N_0 and N_1.

$$
\begin{aligned}
&\approx \frac{C^2 E_0}{(r_d D)^{d-1}} \sum_{i,j=1}^{N_0,N_1} \Pi\left(\frac{t}{\delta} - \frac{r_d + D + R_1^j - R_0^i + \frac{(R_i^i)^2}{2D}}{c\delta}\right) \\
&= \mathcal{A}(r_d, D, d) \sum_{i,j=1}^{N_0,N_1} \Pi\left(\frac{t}{\delta} - \frac{\mathcal{L}(r_d, R_0^i, R_1^j, D)}{c\delta}\right) \qquad (10)
\end{aligned}
$$

where $\mathcal{A}(r_d, D, d) \equiv C^2E_0/(r_dD)^{d-1}$ is the amplitude, and $\mathcal{L}(r_d, R_0^i, R_1^j, D) \equiv r_d + D + R_1^j - R_0^i + (R_i^i)^2/(2D)$ is a phase shift. r_d and D are constant for all terms of the sum. There is constructive interference from all N_1 target scatterers, if the quadratic term in the phase shift $\mathcal{L}$ is negligible small and if there is an i-value where expression $a_1R_0^{i+j} - a_0R_1^j = a_1R_0^i$ for $j = 1, 2, \cdots, N_1$, *-i.e.* if the sequence S_1 is a subsequence of S_0.

Limitations of the double diffraction system. – Equation (9) suggests that the relative intensity I_{max}/N_1^2 is independent of N_1 and N_0. Figure 4 is a contour plot of the relative intensity versus N_0 and N_1, where the parameters are the same as in fig. 2. It shows that the relative intensity is equal to the theoretical value given by eq. (9), $I_{max}/N_1^2 = 10^{-14}$ if the number of target scatterers N_1 is less than the value N_c, and less than half the number of of source scatterers, *-i.e.* $N_1 < \min\{N_c, N_0/2\}$. If $\min\{N_c, N_0/2\} < N_1 < \min\{N_c, N_0\}$ the relative intensity is sometimes equal to the theoretical value and sometimes less. For $\min\{N_c, N_0\} < N_1$ the relative intensity is always less than the theoretical value. If $N_0 < N_1$ then the sequence S_0 is shorter than the sequence S_1, and therefore S_1 can not be a subsequence of S_0. Hence there is no constructive interference from all N_1 scatterers. If $N_0 > 2 * N_1$, S_1 is always a subsequence of S_0, since the recurrence time for PAC sequences is twice the length of the sequence [17], and therefore there is constructive interference from all N_1 target scatterers. In the intermediate region constructive interference may or may not occur. Figure 4 also shows that constructive interference from all N_1 scatterers does not occur if N_1 exceeds the value N_c, no matter how large N_0. This is due to the quadratic term in the phase shift. If the quadratic term for a scatterer exceeds the pulse width, *-i.e.* $(\bar{R}_1^{N_c})^2/(2D) > c\delta$, full constructive interference from all N_1 target scatterers will no longer occur. Therefore, the value N_c can be estimated with

$$\bar{R}_1^{N_c} \approx \sqrt{2Dc\,\delta} \qquad (11)$$

With $\bar{R}_1^{N_1} = N_1a_1\sqrt{1+\tau_1^2}/(1+\tau_1)$ we obtain

$$N_c \approx \sqrt{2Dc\,\delta}\frac{1+\tau_1}{a_1\sqrt{1+\tau_1^2}} \qquad (12)$$

Table 1 shows a comparison between numerical estimates and the theoretical value for several N_1 values.

Table 1: Comparison between theoretical estimates and simulation of N_c

δ	N_c estimated	N_c simulated
0.01	61.55	62±2
.02	87.05	88±2
.03	106.61	108±2

System identification with double diffraction. – The main peak in the diffraction pattern can be used to identify the structure of the target scatterers. Figure 5 shows the height of the main diffraction peak versus the structural parameter of the source scatterers α_0. The number of scatters is $N_0 = 30$ and $N_1 = 15$. The other parameters are the same as in fig. 2. Within the parameter range $0.540 < \alpha_0 < 0.566$ the intensity is constant and the numerical value is very close the the theoretical value given by eq. (9). Hence the numerical estimate of the structural parameter of the target is $\alpha_1 = 0.553 \pm 0.14$. The actual parameter of the source scatterers is $\alpha_1 = \arctan(2/(1+\sqrt{5})) \approx 0.5536$, which is consistent with the numerical estimate.

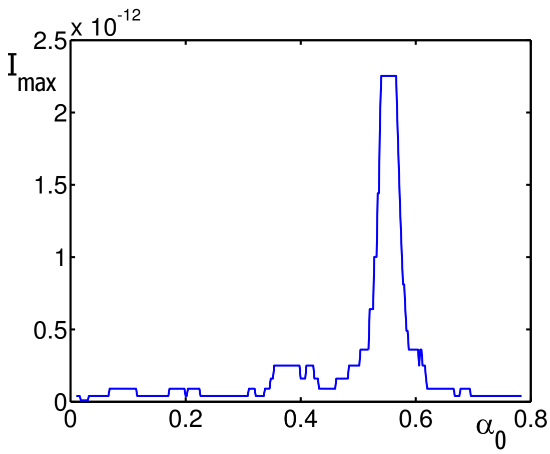

Fig. 5: The intensity of the main peak $I_{max}(\theta_{max})$ versus the structural parameter of the source α_0.

Conclusion. – We have demonstrated that double diffraction can be used to detect the structure of quasiperiodic set of scatterers (see fig. 5). We estimate N_c, the maximum number of the number of target scatterers which contribute to constructive interference, in terms of the width of the original pulse and the distance between two set of scatterers and the structural parameter of the target τ_1 (see eq. (11)). We show that the number of target scatterers which contribute to constructive interference is $N = \min\{N_c, N_1\}$, if the source has at least $2N$ scatterers (see fig. 4). This technique can be applied to analyze the structure of Fibonacci multilayers. In a typical material with quasiperiodic multilayers, the thickness of each layer is on the order of $\bar{l} = 100$ nm, and the number of layers is on the order of 100 [20]. If we use a laser pulse to probe the structure, the length of the pulse has to be at the similar scale, or $c\,\delta \approx 10^{-7}$ m. Therefore, the duration of the pulse δ is at the 100-1000 attosecond range. Attosecond pulses in this range have been observed experimentally in 2001 [21,22]. If the distance between source scatterers and the target scatterers $D = 10$ micron, the critical number of the target scatterers $N_c \approx 140$ (see eq. (12)), which is also within the experimental range. Therefore, it should be possible to determine the structure of quasiperiodic multilayers in a double diffraction experiments with existing technology.

* * *

This research was supported in part by the National Science Foundation Grant DMS 03-25939 ITR.

REFERENCES

[1] D. Shechtman D., Blech I., Gratias D. and J. W. Cahn, *Phys. Rev. Lett.*, **53** (1984) 1951.
[2] Mikulík P., Holý V., Kuběna J. and Ploog K., *Acta Cryst. A*, **51** (1995) 825.
[3] Yamamoto A., *Acta Cryst. A*, **52** (1996) 509.
[4] Merlin R., Bajema K., Clarke R., Juang F. -Y. and Bhattacharya P. K., *Phys. Rev. Lett.*, **55** (1986) 1768.
[5] Wang N., Chen H. and Kuo K. H., *Phys. Rev. Lett.*, **59** (1987) 1010.
[6] Jiang, S. S., Peng R. W., Hu A., Zou J., Cockayne D. J. H. and Sikorski A., *J. Appl. Cryst.*, **30** (1997) 114.
[7] T. Jassen, *Acta Crystallogr. A*, **42** (1986) 216.
[8] Abe E., Yan Y. and Pennycook S. J., *Nature Materials*, **3** (2004) 759.
[9] Plapp B. B. and Hübler A. W., *Phys. Rev. Lett.*, **65** (1990) 2302.
[10] Eisenhammer T., Hübler A., Geisel T. and Lüscher E., *Phys. Rev. A*, **41** (1990) 3332.
[11] Chang K., Kodogeorgiou A., Hübler A. W. and Jackson E. A., *Physicsa D*, **51** (1991) 99.
[12] Krempl S., Eisenhammer T., Hübler A., Mayer-Kress G. and Milonni P. W., *Phys. Rev. Lett.*, **69** (1992) 430.
[13] Wargitsch C. and Hübler A., *Phys. Rev. E*, **51** (1995) 1508.
[14] Arsenault L. E. and Hübler A. W., *Phys. Rev. E*, **51** (1995) 3561.
[15] Hübler A. W., Kuhl U., Wittmann R. and Nagata T., *Chaos*, **7** (1997) 577.
[16] Foster G., Hübler, A. and Dahmen K., *Phys. Rev. E*, **75** (2007) 036212.
[17] Xu J. and Hübler A., *Phys. Rev. B*, **67** (2003) 184202.
[18] Dubost B., Lang J-M., Tanaka M., Sainfort P. and Audier M., *Nature*, **324** (1986) 48.
[19] Janot C., *Quasicrystals, a Primer* (Clarendon Press, Oxford) 1992, p. 23.
[20] Gellermann W., Kohmoto M., Sutherland B. and Taylor P. C., *Phys. Rev. Lett.*, **72** (1994) 633.
[21] Paul P. M., Toma E. S., Breger P., Mullot G., Augé F., Balcou Ph., Muller H. G. and Agostini P., *Science*, **292** (2001) 1689.
[22] Hentschel M., Kienberger R., Spielmann Ch., Reider G. A., Milosevic N., Brabec T., Corkum P., Heinzmann U., Drescher M. and Krausz F., *Nature*, **414** (2001) 509.